Structural and magnetic properties of nanocrystalline ZnFe2O4 powder synthesized by reactive ball milling

Traian Marinca, Ionel Chicinas, Olivier Isnard, Viorel Pop

Structural and magnetic properties of nanocrystalline $ZnFe_2O_4$ powder synthesized by reactive ball milling

T. F. MARINCA, I. CHICINAŞ*, O. ISNARD[a], V. POP[b]
Materials Sciences and Technology Department, Technical University of Cluj-Napoca, 103-105 Muncii Avenue, 400641 Cluj-Napoca, Romania
[a]*Institut Néel, CNRS, Université Joseph Fourier, 25 rue des Martyrs, 38042 Grenoble, France*
[b]*Faculty of Physics, Babes-Bolyai University, 1 M. Kogalniceanu St., 400641 Cluj-Napoca, Romania*

The zinc ferrite ($ZnFe_2O_4$) has been obtained in nanocrystalline state by reactive milling in a high energy planetary mill from a stoichiometric mixture of oxides (ZnO and α-Fe_2O_3). A post milling annealing promotes the solid state reaction, improves the ferrite crystalline state and removes internal stresses. The formation of zinc ferrite was studied by X-ray diffraction and magnetic measurements. The chemical homogeneity and morphology of the powders were studied by X-ray microanalysis and scanning electron microscopy. The mean crystallite size after 16 h of milling was found to be 18 ± 2 nm. The lattice parameter of the obtained ferrite depends on the milling time and subsequent annealing treatment. It is lower than that of zinc ferrite obtained by the ceramic method. The evolution of the magnetization versus milling time is discussed in terms of milling induced cations reorganisation into the spinel structure.

(Received November 15, 2010; accepted January 26, 2011)

Keywords: Reactive milling, Mechanical alloying, zinc ferrite, Nanocrystalline material

1. Introduction

Soft magnetic ferrites are the subject of many researches due to their multiple applications in various industrial fields [1-6]. They also constituted a large playground for fundamental research for several decades. The synthesis routes of soft ferrites are also various: traditional method - ceramic method, sol-gel, co-precipitation, wet milling or dry milling [2, 7-11]. The magnetic properties of soft ferrites are determined by the cations distribution within the crystal structure. The ferrites are soft magnetic materials like $MeO{\cdot}Fe_2O_3$, where Me is a divalent metal like Ni, Fe, Cu, Zn, Mn etc. or a combination of these metals (eg. $(Ni_{1-x}Zn_x)O{\cdot}Fe_2O_3$) [1]. Spinel structure, which is characteristic for soft magnetic ferrites, has two different types of atomic sites on which the cations are localized in the crystal lattice: tetrahedral sites and octahedral sites. In the normal spinel structure, the tetrahedral sites are occupied by Me^{2+} ions and octahedral sites are occupied by Fe^{3+} ions (eg. Zn, Cd ferrites). In the inverse spinel structure, the tetrahedral sites are occupied by Fe^{3+} ions and Me^{2+} ions occupy half the octahedral sites (eg. Fe, Ni, Co ferrites etc). In general, there is not a complete inversion of cations between tetrahedral and octahedral sites in the spinel structure, but a partial inversion which could be written as follows $(Me_{1-x}Fe_x){\cdot}(Fe_{2-x}Me_x)O_4$ [6, 8, 12-15].

The magnetic behaviour of the spinel ferrite is usually ferrimagnetic, with the exception of cadmium and zinc ferrite which are paramagnetic at room temperature [1]. Zinc ferrite is antiferromagnetic at temperatures below 10 K [1, 15]. However, if it is synthesized by unconventional methods, it may present different magnetic ordering [2, 16 - 18]. Another type of magnetic order is given by Fe^{3+} and Zn^{2+} cations inversion in the crystalline structure positions [16 - 18]. One way to cause the inversion of the cations is mechanical milling. Even when starting from a mixture of oxides to obtain zinc ferrite by mechanical milling or from a polycrystalline ferrite obtained by other methods, the cations inversion can be induced by milling [19-25]. Nanocrystalline zinc ferrite was obtained by mechanical milling from a commercial powder of polycrystalline zinc ferrite. The inversion of the cations between the tetrahedral and octahedral sites in the cubic spinel structure has been reported [25]. The grain size is found to decrease with increasing milling time [4, 24-25]. Nanocrystalline zinc ferrite has been obtained from a stoichiometric mixture of ZnO and Fe_2O_3 [3, 5-6, 12]. After 6 hours of milling, zinc ferrite was obtained and iron contamination has been observed [3]. Other authors reported a superparamagnetic behaviour for the milled $ZnFe_2O_4$ samples and the cations inversion [17]. In addition, a spin canted effect and ionic disorder were observed and these phenomenon were attributed to the effect of milling [6, 13, 18].

The present paper presents the synthesis of nanocrystalline zinc ferrite by reactive milling and the characterization of some structural, morphological and magnetic properties.

2. Experimental

A stoichiometric mixture of commercial oxides (Alfa Aesar), ZnO - zincite and α-Fe_2O_3 – hematite, was used to obtain the nanocrystalline zinc ferrite by high energy

reactive milling (RM). The starting mixture (starting sample – SS) was containing high purity powders (99.99%). It has been homogenised 15 minutes in a Turbula type blender and than was milled in air atmosphere, using a Pulverisette 4 (Fritsch) planetary ball mill. Stainless steel vials with 250 cm^3 volume and stainless steel balls with 15 mm diameter were used for the milling process. The ball to powder mass ratio (BPR) was 15: 1. The vial rotational speed (ω) and the disc rotational speed (Ω) were established at 800 rpm, respectively at -400 rpm during the entire period of milling. Several milling times were used ranging from 4 h up to 30 h. After milling, the samples were subjected to a heat treatment under vacuum at a temperature of 350 °C for 4 hours (TT). The annealing has a double effect: (i) improvement of the solid-state reaction of ferrite formation and (ii) diminution of the internal induced buring milling.

The formation of zinc ferrite during milling was studied by X-ray diffraction using a Siemens D5000 diffractometer operating in reflection with CoKα radiation (λ = 1.7903 Å). The X-rays diffraction patterns were recorded in the angular range 2θ = 20 - 90°. The mean crystallite size was calculated applying Scherrer's formula to the annealed samples [26]. The calculation of cell parameters was performed using the X-ray diffraction and refined by the software Celref 3 [27].

The particle morphology and the local chemical homogeneity were investigated by scanning electron microscopy (SEM) using a microscope JEOL - JSM 5600-LV which is equipped with an EDX spectrometer (Oxford Instruments, INCA 200 soft). The particles size distribution, before and after milling, has been determined using a Laser Particle Size Analyzer (Fritsch Analysette 22 – Nanotec), with an analysis field of 10 nm - 2000 μm.

The magnetization curves, M(H), were recorded at room temperature using the extraction sample method in a continuous magnetic field of up to 8 T [28].

3. Results and discussion

The Bragg peaks positions for as-milled samples and for milled and subsequently annealed samples are shown in Fig. 1. For each phase the positions of the Bragg peaks are indicated in the Fig. 1. The positions of the Bragg peaks for the as-milled, milled and subsequently annealed powders are compared with a reference sample consisting of the starting powder (stoichiometric mixture of elemental oxides). For the starting sample, the observed Bragg peaks corresponds to zincite (ZnO) and hematite phases (α-Fe_2O_3).

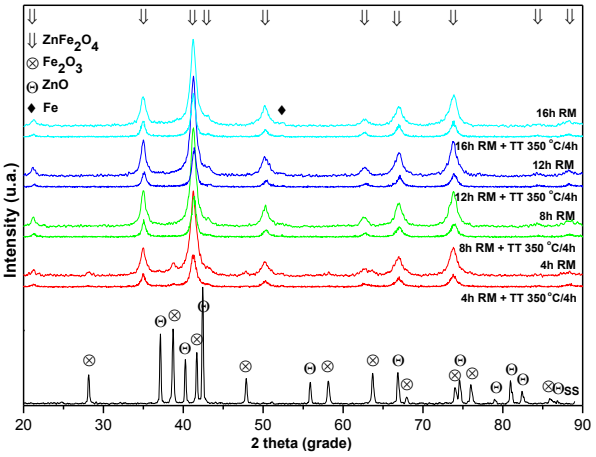

Fig. 1. XRD patterns of the as-milled samples (4, 8, 12, 16 h), of the samples milled and subsequently annealed at 350 °C for 4 h. The starting sample is noted by ss. For clarity, the spectra have been shifted vertically. The XRD maxima for different phases are shown.

After 4 hours of milling the disappearance of the Bragg peaks corresponding to the zincite phase is observed as well as a decrease in intensity of the hematite peaks and the appearance of new Bragg peaks, which correspond to the zinc ferrite phase. The disappearance of Bragg peaks corresponding to the zincite phase is the result of the atomic diffusion in the structure of the hematite phase to form the zinc ferrite or the result of the transformation of crystalline zincite to the amorphous state during milling [3, 29, 30]. For this milling time we have a transformation of the oxides into the zinc ferrite with a small amount of oxide powders unreacted. It can be also noticed a small contamination of the powder with iron from the vial and balls. The powders contamination with elements from the milling bodies is a phenomenon difficult to avoid completely and frequently encountered [3]. The amount of hematite that remains unreacted is estimated at about 10 % and the amount of iron from contamination is 2-3%.

After 8 hours of milling, only the peaks that correspond to the zinc ferrite phase and a small peak corresponding to iron (which is a result of contamination) are observed. For this time of milling it can be considered that the zinc ferrite is formed. Similar results were reported in references [3, 30]. For milling times of 12 and 16 hours the Bragg peaks of the zinc ferrite and iron phases can be observed. The peaks are larger than for the eight hours of milling. This is a consequence of the fact that the second order internal stresses induced in the samples are greater and the grain size is reduced by milling [2, 16].

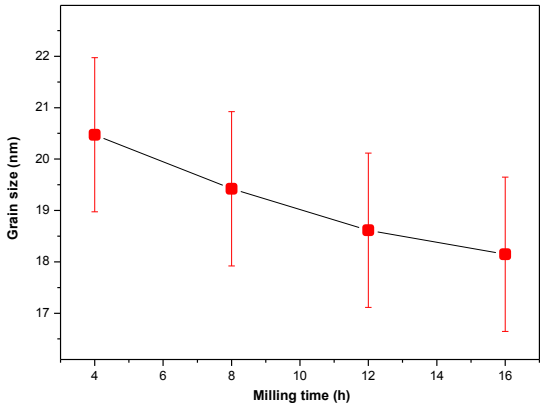

Fig. 2. Evolution of mean crystallite size as a function of milling time.

The annealing improves the ferrite spinel structure and removes the internal stresses induced in the samples On the other hand, the annealing improves the ferrite phase formation, but doesn't complete the reaction between the un-reacted oxides for 4 h of milling. The Bragg reflections corresponding to hematite phase are still observed in the diffraction patterns. For the 4 h milled and annealed sample an amount of 6 % of hematite was found.

The evolution of mean crystallite size versus milling time (for as-milled and milled and subsequently annealed samples) is shown in Fig. 2. After only 4 hours of milling, zinc ferrite is not formed completely, but the mean crystallite size is already in nanoscale region. The mean crystallites size decreases slowly with increasing the milling time from 20 ± 2 nm to 18 ± 2 nm during of 12 hours of milling.

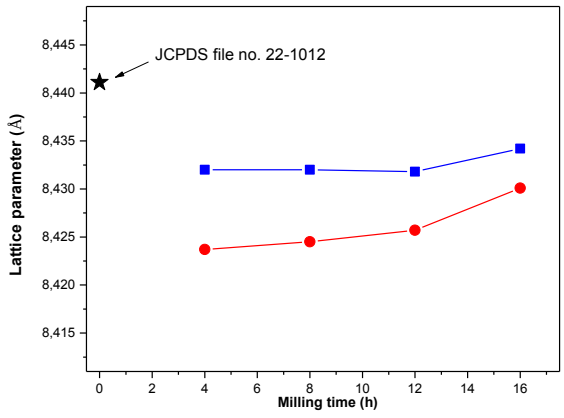

Fig. 3 Evolution of lattice parameter versus milling time for the as-milled samples and for the milled and subsequently annealed samples. The value for the lattice parameter from JCPDS file no. 22 – 1012 (reference ceramic sample) is also indicated.

The evolution of the lattice parameter versus the milling time is presented in Fig. 3. It can be observed a difference between the calculated lattice parameter for the as-milled samples and the lattice parameter calculated for the annealed samples. The lattice parameter for the as-milled samples is larger than that of the milled and subsequently annealed samples. This difference is related to the existence of the second order internal stresses induced by milling. After annealing the lattice parameter decreases due the lattice relaxation. The lattice parameter is lower compared to that of the zinc ferrite obtained by the ceramic method (0.84411 nm, JCPDS file no. 22-1012), but it is comparable with the values reported in the literature [20, 30]. A lower lattice parameter could indicate an inversion of cations between the tetrahedral and octahedral sites in the spinel structure.

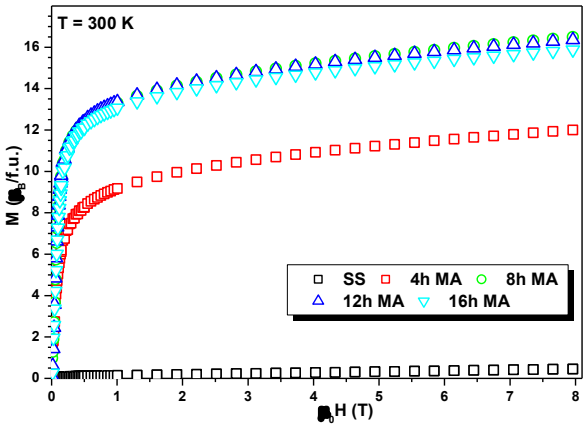

Fig. 4. Magnetisation curves at 300 K for the as-milled samples and for the starting sample.

The magnetization curves also reflect a change in the structure of the starting powders (Fig. 4). In comparison with the starting mixture, after 4 hours of milling, the magnetization curves of the new phase formed by milling are exhibiting different magnetic behaviour. The zinc ferrite obtained by ceramic method has a paramagnetic behaviour at 300 K, as it was mentioned above. For the zinc ferrite obtained by reactive milling a change of the configuration of the cations in spinel structure sites may occurs, which could explain the change of magnetic properties [20-24]. In a normal spinel structure Fe^{3+} cations are ordered in the octahedral sites and Zn^{2+} cations in the tetrahedral sites. By milling we induce a partially inversed distribution of the Fe^{3+} and Zn^{2+} cations between octahedral and tetrahedral sites in the spinel structure. Consequently the cations have non-equilibrium distribution and a change in the magnetic properties occurs. This could explain the observed magnetic behaviour. A ferrimagnetic ordering induced by mechanical milling in the zinc ferrite spinel structure, was also reported in Refs. [4, 24-25].

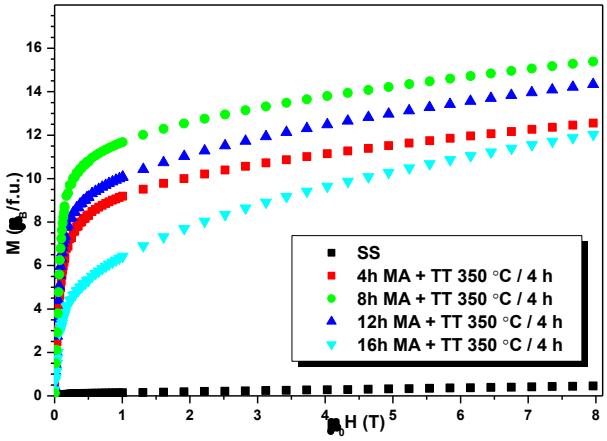

Fig. 5. Magnetisation curves at 300 K for the milled and subsequently annealed samples and for the starting sample.

It may be also noted that the magnetization is not saturated even for an applied magnetic field of 8 T. The difficulty to saturate the magnetization could be due to a particular configuration of the magnetic spins (spin canted) or to a superparamagnetic behaviour of the very small particles [6, 13]. The results of magnetic measurements obtained on samples milled and annealed at 350 °C under vacuum for 4 hours are shown in Fig. 5. A decrease of the magnetization value is observed upon annealing for all samples. The magnetization decreases after annealing due to the reorganization of the iron and zinc cations between octahedral and tetrahedral sites and because of the lattice relaxation [4-5, 31]. The magnetization is lower for larger milling time, so it can be assumed that the cations re-ordering is higher for the samples milled for longer time due the fact that by increasing the milling time the system will be farer from equilibrium.

The particles size distribution for the starting powder and for the 16 hours milled sample is shown in Fig. 6. It can be observed that the particles sizes of the 16 hours milled sample are bigger in comparison with those of the starting sample. The particles sizes analysis revealed that for all milled samples the particles sizes are below 40 micrometers. The median particle diameter (D_{50}) is 5.3 microns for the 16 hours milled sample.

The images obtained by scanning electron microscopy for the starting sample, 8 hours milled sample and 16 hours milled sample are shown in Fig. 7a – 7f. The micrometer-sized particles of the starting mixture are easily seen. The particles sizes observed by SEM are less than 4 microns in accordance with manufacturer's specifications. The milled powders are formed from agglomerated particles, having a polyhedral shape (Fig. 7c - 7f).

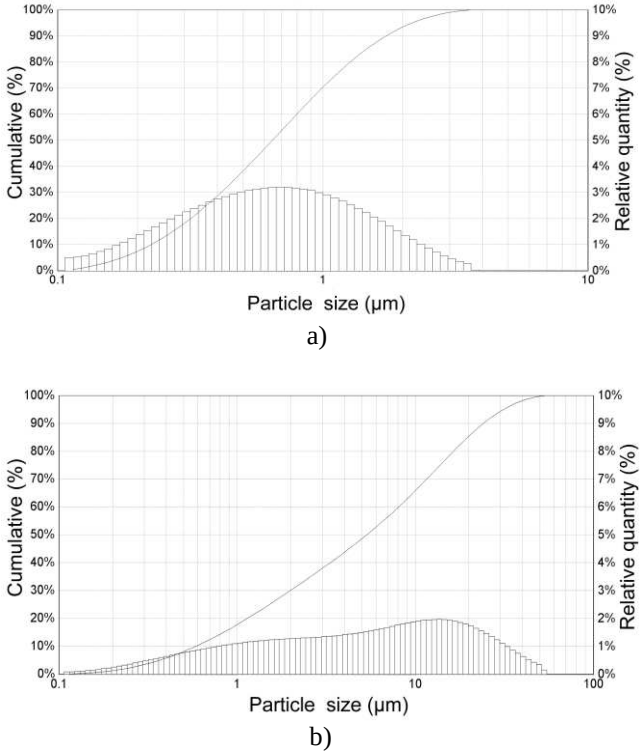

Fig. 6. Particles size distribution obtained by laser particle size analyser for the: the starting mixture a) and for the 16 hours milled sample b).

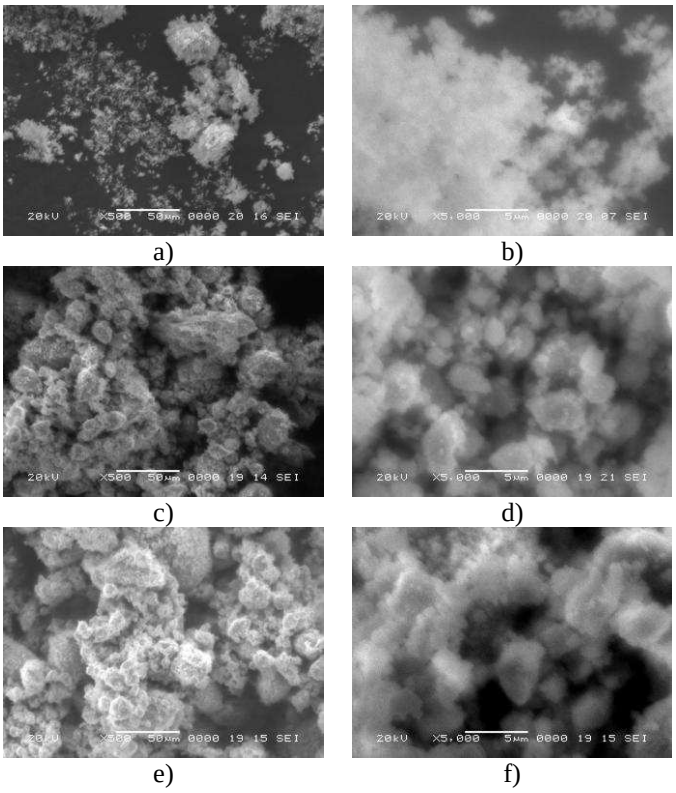

Fig. 7. Particles morphology for the: starting powder a) and b), 8 hours milled sample c) and d), 16 h milled sample e) and f). SEM images; magnification is 500 X and 5000X to the left and right respectively.

The X-rays microanalysis (EDX) revealed a good homogeneity of the powders in the starting mixture, although some areas are richer in one element or another. The local chemical homogeneity of the elements in the samples increases with milling time [29].

4. Conclusion

Nanocrystalline zinc ferrite was obtained as single phase after 8 hours of reactive milling from a stoichiometric mixture of the commercial iron and zinc oxides. The annealing improves the solid state reaction of the zinc ferrite formation and removes the second order internal stresses. The mean crystallite size is typically of nanometric scale at 4 hours of milling and decreases with increasing milling time. A mean crystallite size of 20 ± 2 nm was found after 8 hours of milling. The lattice parameter of the obtained ferrite increases versus milling time, but is lower than that of the ferrite obtained by the classical ceramic method. The lattice parameter for the milled and subsequently annealed sample decreases, due to the lattice relaxation during annealing.

The magnetization studies suggest an inversion of the Fe^{3+} and Zn^{2+} cations between the tetrahedral and octahedral sites in the spinel structure. The magnetization was not saturated even under a magnetic field of 8 T. This behaviour could be explained by a superparamagnetic component that can be given by very small particles or by a spin canted effect.

The particles of the milled powders are agglomerated and have a polyhedral shape.

Reactive ball milling method is suitable to obtain nanocrystalline zinc ferrite with good magnetic properties. Further investigations in order to clarify the cations distribution are in progress.

Acknowledgment

This work was supported by CNCSIS – UEFISCSU, project number PNII – IDEI code 1519/2008.

References

[1] B. D. Cullity, C. D. Graham, Introduction to Magnetic Materials, Second Edition, IEEE Press&Wiley, New Jersey, (2009).
[2] S. Ozcan, B.Kaynar, M. M. Can, T. Fırat, Mater. Sci. Eng., B **121**, 278 (2005).
[3] T. Verdier, V. Nachbaur, J. Malick, J. Solid State Chem. **178**, 3243 (2005).
[4] V. Šepelák, L. Wilde, U. Steinike, K.D. Becker, Mater. Sci. Eng., A **375–377**, 865 (2004).
[5] D. Arcos, N. Rangavittal, M. Vasquez, Mater. Sci. Forum **269-272**, 87 (1998).
[6] G. F. Goya, H. R. Rechenberg, Mater. Sci. Forum **403**, 127 (2002).
[7] F. J. C. M. Toolennar, J. Mater. Sci. **24**, 1089 (1989).
[8] M. J. Akhtar, M. Nadeem, S. Javaid, M. Atif, J. Phys.: Condens. Matter. **21**, 405 (2009).
[9] V. Berbenni, C. Milanese, G. Bruni, A. Marini, I. Pallecchi, Thermochim. Acta **447**, 184 (2006).
[10] M. Gaudon, N. Pailhe, A. Wattiaux, A. Demourgues, Mater. Res. Bull. **44**, 479 (2009).
[11] J. A. Gomes, M. H. Sousa, F. A. Tourinho, J. Mestnik-Filho, R. Itri, J. Depeyrot, J. Metastable Nanocryst. Mater. **20-21**, 617 (2004).
[12] W. Kim, F. Saito, Powder Technol. **114**, 12 (2001).
[13] G. F. Goya, H. R. Rechenberg, M. Chen, W. B. Yelon, J. Appl. Phys. **87**, 11 (2000).
[14] S. D. Shenoy, P. A. Joy, M. R. Anantharaman, J. Magn. Magn. Mater. **269**, 217 (2004).
[15] C. Upadhyay, H. C. Verma, V. Sathe, A. V. Pimpale, J. Magn. Magn. Mater. **312**, 271 (2007).
[16] C. N. Chinnasamy, A Narayanasamy, N Ponpandian, K Chattopadhyay, H Guerault, J-M Greneche, J. Phys.: Condens. Matter. **12**, 7795 (2000).
[17] C. N. Chinnasamy, A. Narayanasamy, N. Ponpandian, K. Chattopadhyay, H. Guerault, J-M. Greneche, Scripta Mater. **44**, 1407 (2001).
[18] G. F. Goya, H. R. Rechenberg, J. Magn. Magn. Mater. **196-197**, 191 (1999).
[19] H. Yang, X. Zhang, C. Huang, W. Yang, G. Qiu, J. Phys. Chem. Solids **65**, 1329 (2004).
[20] F. S. Li, L. Wang, J. B. Wang, Q. G. Zhou, X. Z. Zhou, H. P. Kunkel, G. Williams, J. Magn. Magn. Mater. **268**, 332 (2004).
[21] Vladimír Šepelák, Peter Druska and Ursula Steinike, Materials Structure, **6**, 2 (1999).
[22] C. N. Chinnasamy, A. Narayanasamy, N. Ponpandian, K. Chattopadhyay, Mater. Sci. Eng. A **304–306**, 983 (2001).
[23] V. Šepelák, L. Wilde, U. Steinike, K. D. Becker, Mater. Sci. Eng. A **375–377**, 865 (2004).
[24] H. Ehrhardt, S. J. Campbell, M. Hofmann, J. Alloys Compds. **339**, 255 (2002).
[25] M. Hofmann, S. J. Campbell, H. Ehrhardt, R. Feyerherm, J. Mater. Sci. **39**, 5057 (2004).
[26] P. Scherrer, Nachr. Gött. Matematisch Phys. Klasse, **I**, 98 (1918).
[27] J. Laugier, B. Bochu, LMGP-SUITE, Suite of programs for the interpretation of X-ray experiments, ENSP/Laboratoire des Matériaux et du Génie Physique/BP46 38082 Saint Martin d'Hère-France. http://www.inpg.fr/LMGP.
[28] A. Barlet, J. C. Genna, P. Lethuillier, Cryogenics, **31**, 801 (1991).
[29] T. F. Marinca, I. Chicinaş, C. V. Pricǎ, F. Popa, B. V. Neamţu, O. Isnard, Mater. Sci. Forum, (2010) in press.
[30] T. Verdier, V. Nivoix, M. Jean, J. Mater. Sci. **39**, 5151 (2004).
[31] V. Šepelák, S. Wiβmann, K. D. Becker, J. Magn. Magn. Mater. **203**, 135 (1999).

*Corresponding author: Ionel.Chicinas@stm.utcluj.ro